

**Title:** SpeedMixing: Rapid Synthesis and Discovery of Model Pharmaceutical Cocrystals without Milling or Grinding Media

**Authors:** Yong Teoh,<sup>a</sup> Ghada Ayoub,<sup>a</sup> Igor Huskić,<sup>a</sup> Hatem M. Titi,<sup>a</sup> Christopher W. Nickels,<sup>b</sup> Brad Herrmann,<sup>b</sup> Tomislav Friščić\*<sup>a</sup>

**Addresses:** a) Department of Chemistry, McGill University, 801 Sherbrooke St. W. H3A 0B8 Montreal, Canada; b) Flacktek Inc. 1708 SC-11, Landrum, SC 29356, United States

**Corresponding author e-mail:** tomislav.friscic@mcgill.ca

**Abstract:** We present SpeedMixing, a rapid blending technology, as an approach for the mechanochemical discovery and synthesis of model pharmaceutical cocrystals without the need for bulk solvents and milling/grinding media. The syntheses of well-known model pharmaceutical cocrystals based on the active pharmaceutical ingredients (APIs) carbamazepine, dihydrocarbamazepine, and nicotinamide demonstrate SpeedMixing as a method for rapid, scalable, and selective synthesis of cocrystals, cocrystal polymorphs and stoichiomorphs, including the discovery of an unexpected methanol solvate of the archetypal cocrystal of carbamazepine and saccharin, which has eluded numerous and extensive screens reported over almost 20 years.

### Main text

Mechanochemical transformations, typically conducted by milling, grinding or extrusion, have attracted attention as methods for synthesis and screening of pharmaceutical solid forms (e.g. polymorphs, cocrystals, salts), as well as the synthesis of pharmaceutical fragments and individual active pharmaceutical ingredients (APIs).<sup>[1-3]</sup> Such transformations, which can be conducted neat or, more effectively, in the presence of a small or catalytic amount of a liquid additive (e.g. liquid-assisted grinding, LAG),<sup>[4]</sup> offer a wide range of attractive opportunities for synthesis and screening. These include speed, high screening efficiency, ability to screen for new materials independent of relative solubilities of starting materials, and the overall absence of bulk solvents.<sup>[4,5]</sup> A major concern behind such processes, however, is the need for grinding, milling or extrusion media that can actively participate in the transformation and produce unwanted contamination through abrasion or chipping.<sup>[6]</sup> Such considerations have inspired the recent search for media-free approaches for mechanosynthesis, including ageing of materials in humid air or vapors of organic solvents (e.g. accelerated ageing), enabling the preparation of cocrystals, APIs and metal-organic frameworks.<sup>[7]</sup>

Here we present a novel technique for media-free synthesis of pharmaceutical cocrystals in the absence of bulk solvents and milling media, achieved by rapid spinning of cocrystal components using SpeedMixing, a dual asymmetric centrifugal (DAC) mixing technology (Figure 1a) developed for mixing of viscous materials and powder blending.<sup>[8]</sup> We show the ability to use SpeedMixing for rapid (minutes) and scalable (at least tens of grams) synthesis of model pharmaceutical cocrystals, including selective synthesis of polymorphs, stoichiomorphs, and the discovery of novel phases. In particular, SpeedMixing revealed the unexpected existence of a methanol solvate of the archetypal pharmaceutical cocrystal of carbamazepine (**CBZ**) and saccharin (**SAC**): this appears to be the first reported solvate in this cocrystal system, which is

particularly surprising considering that **CBZ**·**SAC** has been extensively studied and regularly used as a pharmaceutical cocrystal model for almost 2 decades.<sup>9,10</sup>

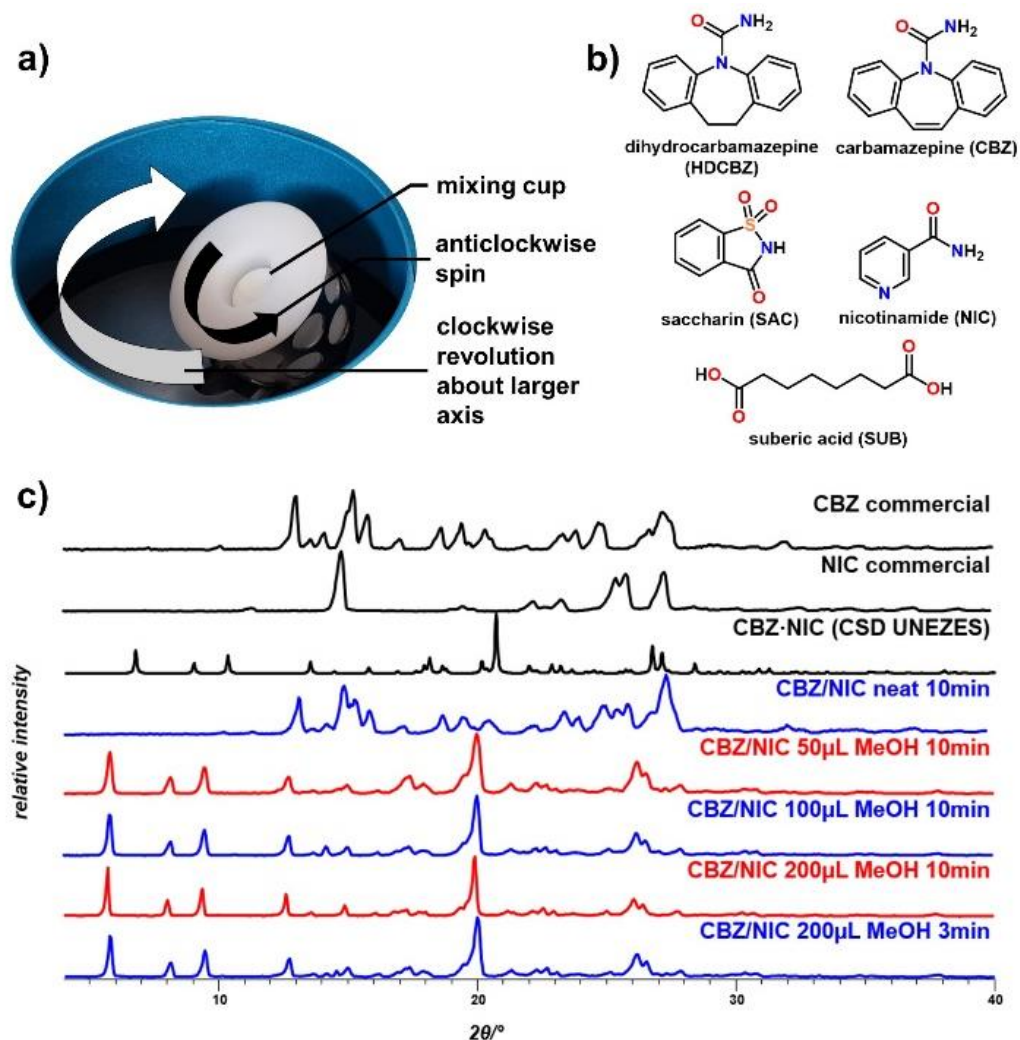


**Figure 1.** a) Picture of a Flacktek SpeedMixer spinning station: the cup spins in a clockwise fashion while also revolving anticlockwise around a central axis; b) cofomers and APIs used in this study; c) selected PXRD patterns for SpeedMixing synthesis of the **CBZ**·**NIC** cocrystal, revealing complete conversion in the presence of 200  $\mu$ L MeOH ( $\eta = 0.56 \mu\text{L}/\text{mg}$ ) on a 1 mmol (358 mg) scale, at 3000 rpm (top-to-bottom): reactants **CBZ** (Form III) and **NIC**, simulated for **CBZ**·**NIC** (CSD UNEZES), a 1:1 stoichiometric mixture of **CBZ** and **NIC** after 10 min SpeedMixing neat, 1:1 stoichiometric mixtures of **CBZ** and **NIC** after 10 min SpeedMixing with 50 ( $\eta = 0.14 \mu\text{L}/\text{mg}$ ), 100 ( $\eta = 0.28 \mu\text{L}/\text{mg}$ ) and 200  $\mu$ L MeOH ( $\eta = 0.56 \mu\text{L}/\text{mg}$ ), and a mixture of **CBZ** and **NIC** after 3 min SpeedMixing with 200  $\mu$ L MeOH ( $\eta = 0.56 \mu\text{L}/\text{mg}$ ).

All experiments were done using a Flacktek SpeedMixer, which uses DAC technology and was recently used for exfoliation of cellulose.<sup>[8]</sup> In SpeedMixing, the sample simultaneously rotates around a central axis at a high rate, typically up to 3,500 rpm, and revolves around its own axis. In the herein developed SpeedMixing cocrystallization approach, a mixture of cocrystal components is placed in an angled polypropylene cup which is then spun clockwise around a central axis while

rotating counterclockwise (Figure. 1a). In a typical experiment, the reaction mixture is loaded into a cup of 10, 25, or 60 mL volume, pre-mixed by SpeedMixing for 20 seconds at a rate of 3000 rpm, followed by addition of a small amount of a liquid. The quantity of the liquid additive was consistent to that in liquid-assisted mechanochemical techniques, with the  $\eta$  parameter – defined as the ratio of liquid volume (in  $\mu\text{L}$ ) to the weight of the reaction mixture (in mg), in the range of ca. 0.1–1.5  $\mu\text{L}/\text{mg}$ .<sup>[4]</sup> In developing the SpeedMixing approach to pharmaceutical cocrystals, we focused on liquid additives acceptable in pharmaceutical manufacturing: methanol (MeOH), ethanol (EtOH), and water.<sup>11</sup> SpeedMixing was performed either in a single cycle of up to 5 minutes, or in multiple 5-minute cycles separated by three minute periods. Products were all microcrystalline powders, characterized immediately and without prior purification by powder X-ray diffraction (PXRD), Fourier transformation infrared attenuated total reflectance spectroscopy (FTIR-ATR), differential scanning calorimetry (DSC) and thermogravimetric analysis (TGA) in nitrogen gas, and in some cases also by <sup>13</sup>C magic-angle spinning cross-polarisation (CP-MAS) solid-state nuclear magnetic resonance spectroscopy (ssNMR) and scanning electron microscopy (SEM).

As a first trial of cocrystallisation via SpeedMixing, we probed the reaction between the API **CBZ** and nicotinamide (**NIC**, Vitamin B6), anticipated to form the known pharmaceutical cocrystal **CBZ·NIC** (CSD UNEZES).<sup>12</sup> The parameters affecting cocrystallisation rates investigated are volume of liquid additives, mixing speeds, and time. Neat mixing of **CBZ** and **NIC** powders did not lead to cocrystal formation, with the PXRD pattern of the reaction mixture exhibiting Bragg reflections of solid reactants (Figure. 1d). Next, we explored SpeedMixing in presence of a small amount of MeOH (50  $\mu\text{L}$ ,  $\eta = 0.14 \mu\text{L}/\text{mg}$ ), which led to the near complete formation of **CBZ·NIC** in two SpeedMixing cycles. Increasing the MeOH volume to 200  $\mu\text{L}$  ( $\eta = 0.56 \mu\text{L}/\text{mg}$ ) led to complete conversion. While full conversion was observed within two SpeedMixing cycles at either 1000, 2000, 3000 and 3500 rpm, incomplete formation of **CBZ·NIC** was seen at 500 rpm (see ESI).

Next, we targeted the well-known cocrystal of **CBZ** and saccharin (**SAC**). Introduced by Zaworotko in 2003, **CBZ·SAC** occupies a central place as a model pharmaceutical cocrystal in many studies,<sup>9,10</sup> and provides an opportunity to explore SpeedMixing for selective polymorph synthesis. There are two known polymorphs of **CBZ·SAC**, the thermodynamically stable Form I (CSD UNEZAO) and the metastable Form II (CSD UNEZAO01).<sup>9,13</sup> Similar to **CBZ·NIC**, neat mixing of a 1:1 stoichiometric mixture of **CBZ** and **SAC** did not lead to cocrystal formation. SpeedMixing with MeOH, however, yielded a material whose PXRD pattern was different from any polymorph, hydrate or MeOH solvate forms of **CBZ**, **SAC**, and **CBZ·SAC** found in the Cambridge Structural Database (CSD) (Figure 2a).<sup>14</sup> Subsequent TGA revealed a loss of weight of ca. 5.4% around 70 °C (Figure 2b), which could be consistent with a solvate of tentative composition **CBZ·SAC·MeOH** (calculated MeOH content: 7.1%).

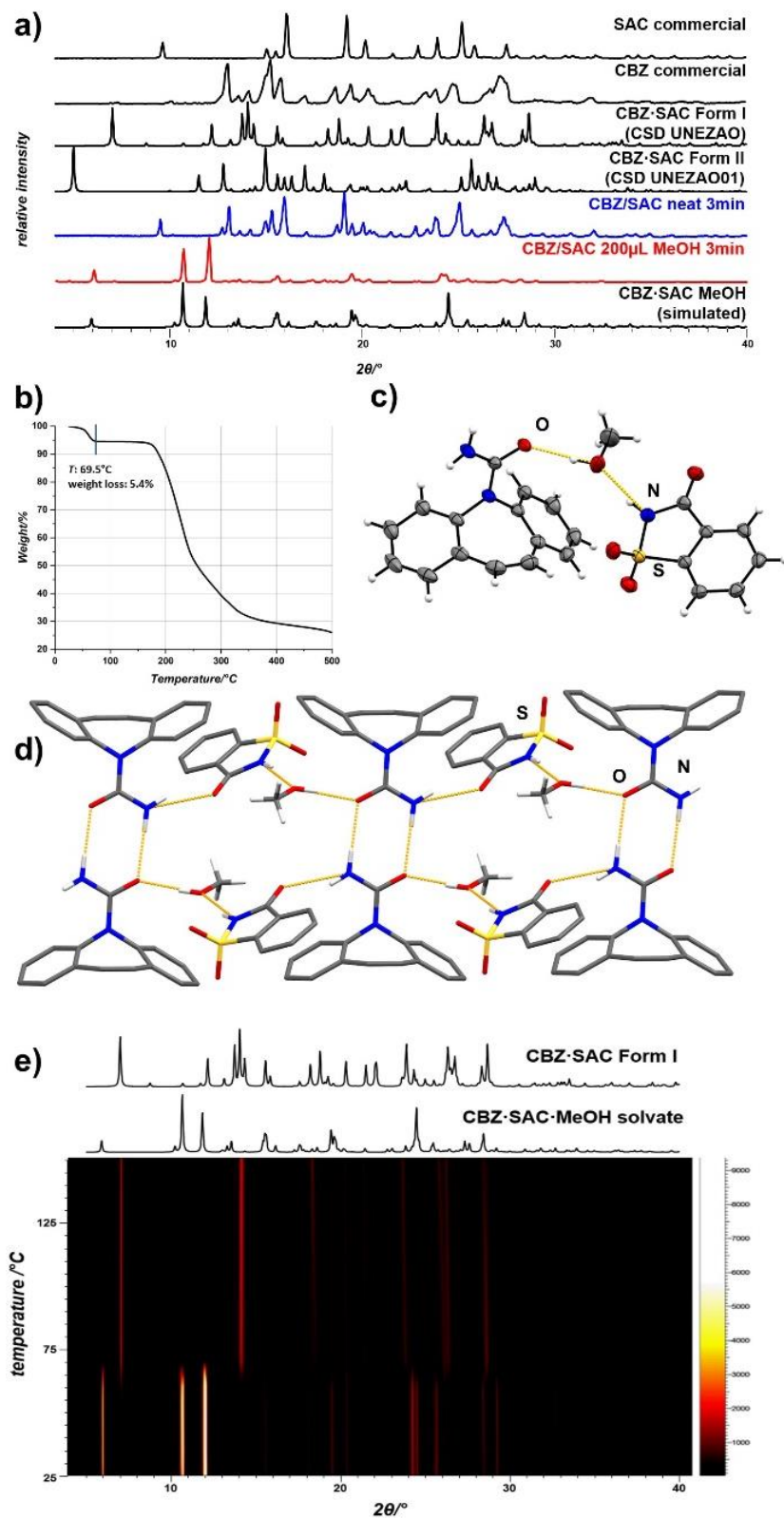


**Figure 2.** (a) Selected PXRD patterns for the SpeedMixing synthesis of **CBZ·SAC·MeOH** (top-to-bottom): reactants **SAC** and **CBZ** (Form III), simulated for **CBZ·SAC** Form I (CSD UNEZAO) and Form II (CSD UNEZAO01), 1:1 stoichiometric mixture of **CBZ** and **SAC** after 3 min SpeedMixing neat, with 200  $\mu$ L MeOH ( $\eta = 0.48 \mu\text{L}/\text{mg}$ ), and

simulated for **CBZ·SAC·MeOH**. (b) Thermogram of **CBZ·SAC·MeOH**; (c) view of the asymmetric unit of **CBZ·SAC·MeOH** crystal structure, with non-hydrogen atoms shown as ellipsoids at 50% probability of electron density; (d) fragment of the crystal structure of **CBZ·SAC·MeOH**, illustrating a hydrogen-bonded tape along the crystallographic *b*-axis. (e) Temperature-resolved *in situ* X-ray powder diffractogram of **CBZ·SAC·MeOH**, demonstrating conversion to **CBZ·SAC** Form I at ~69 °C. Crystallographic data for **CBZ·SAC·MeOH** in CIF format has been deposited with the Cambridge Crystallographic Data Centre (deposition number 2166572).

**Table 1.** Outcomes of SpeedMixing cocrystallisation of **CBZ** and **SAC** in the presence of different volumes (*V*, in  $\mu\text{L}$ ) of either MeOH or different MeOH:H<sub>2</sub>O mixtures as the liquid additive. The  $\eta$  value is also provided for each system, and the ratios of MeOH to H<sub>2</sub>O are based on volume.

<i>V</i> ( $\mu\text{L}$ )	$\eta$ ( $\mu\text{L}/\text{mg}$ )	MeOH	5:1 MeOH: H <sub>2</sub> O	3:1 MeOH: H <sub>2</sub> O	2:1 MeOH: H <sub>2</sub> O	1:1 MeOH: H <sub>2</sub> O	1:2 MeOH: H <sub>2</sub> O	1:3 MeOH: H <sub>2</sub> O	1:5 MeOH: H <sub>2</sub> O
500	1.19	<b>CBZ·SAC·MeOH</b>	Form I	Form I	Form I	Form II	Form II	Form II, <b>CBZ·2H<sub>2</sub>O</b>	<b>CBZ·2H<sub>2</sub>O</b>
200	0.48	<b>CBZ·SAC·MeOH</b>	I, trace II	Form I	Form I	Form II	Form II	Form II, <b>CBZ·2H<sub>2</sub>O</b>	Form II, <b>CBZ·2H<sub>2</sub>O</b>
100	0.24	<b>CBZ·SAC·MeOH</b>	Form I	I, trace II	Form II, trace I	Form II	Form II	Form II, <b>CBZ·2H<sub>2</sub>O</b>	<b>CBZ·2H<sub>2</sub>O</b>
50	0.12	<b>CBZ·SAC·MeOH</b> trace I	Form I, II	Form II, trace I	Form II, trace I	Form II	Form II	<b>CBZ·2H<sub>2</sub>O</b> , trace II	<b>CBZ·2H<sub>2</sub>O</b>

The presence of MeOH in the product was also supported by <sup>13</sup>C CP-MAS ssNMR (see ESI) which revealed a resonance at 49 ppm, consistent with the methyl group carbon of the MeOH molecule.<sup>15</sup> Recrystallisation from anhydrous MeOH provided single crystals suitable for X-ray crystal structure analysis, which verified the discovery of a MeOH solvate of **CBZ·SAC** (Figure 2c).

The new form **CBZ·SAC·MeOH** crystallizes in the *P*-1 space group and exhibits hydrogen-bonded tapes (Figure 2d) of **CBZ** dimers bridged to each other through molecules of **SAC** and MeOH. Within a tape, each MeOH molecule acts as a donor of an O-H···O hydrogen bond to the neighboring **CBZ** dimer (O···O separation 2.724(2) Å), and an acceptor of an N-H···O hydrogen bond from the adjacent **SAC** molecule (N···O separation 2.679(2) Å). Similarly, each **SAC** molecule in a tape participates as an acceptor in an N-H···O hydrogen bond to a neighboring **CBZ** dimer (N···O separation 2.977(2) Å). The overall hydrogen-bonding pattern within each tape can be described as a combination of a  $C_3^3(10)$  chain with  $R_2^2(8)$  and  $R_8^6(20)$  ring supramolecular synthons.<sup>16</sup> The structure of **CBZ·SAC·MeOH** shows similarities to those of **CBZ·SAC** Forms I and II, which exhibit the presence of **CBZ**  $R_2^2(8)$  dimers and chains of hydrogen-bonded **CBZ** and **SAC** molecules, respectively. Upon heating, **CBZ·SAC·MeOH** loses MeOH around 69 °C and transforms into **CBZ·SAC** Form I, as revealed by variable-temperature PXRD analysis (Figure 2e). Analysis of **CBZ·SAC·MeOH** by DSC in a sealed Al pan revealed a broad endothermic signal with a maximum at 68 °C (see SI), which was integrated to measure the **CBZ·SAC·MeOH** enthalpy of desolvation of 25.4 kJ/mol.

Based on a search of the CSD, **CBZ·SAC·MeOH** represents the first reported solvate of the **CBZ·SAC** cocrystal, and this led us to investigate the possible formation of other **CBZ·SAC** solvates by SpeedMixing. While a cursory screen using a set of solvents (CF<sub>3</sub>CH<sub>2</sub>OH, CH<sub>3</sub>CN, *n*-BuOH, toluene, ethyleneglycol, CH<sub>3</sub>NO<sub>2</sub>, see SI) did not reveal any new forms of the **CBZ·SAC**, we observed the known **CBZ·CF<sub>3</sub>CH<sub>2</sub>OH** solvate (CSD SAPDUJ)<sup>17</sup> as an intermediate in the formation of **CBZ·SAC** Form I (see SI). These experiments also revealed rapid formation of

**CBZ**·**SAC** upon SpeedMixing, sometimes within 1 minute (see SI). We also expanded our screen to the related API dihydrocarbamazepine (**DHCBZ**), known to form structurally similar cocrystals to **CBZ**.<sup>18</sup> However, no new forms were observed beyond the known cocrystal **DHCBZ**·**SAC** (CSD OTESEM, see SI).<sup>19a</sup>

Observation of the **CBZ**·**SAC**·MeOH is highly surprising, considering that extensive previously reported solution, slurry, mechanochemical and other screens involving MeOH, including the determination of the phase diagram of the ternary system of **CBZ**, **SAC** and MeOH, never reported the formation of any other cocrystal forms except **CBZ**·**SAC** polymorphs I or II.<sup>19-22</sup> We note, however, that growth of single crystals of **CBZ**·**SAC**·MeOH required the use of anhydrous MeOH as a solvent, while analogous experiments using conventional laboratory MeOH all produced Form I **CBZ**·**SAC**. These observations suggest that the absence of water is an important parameter for the observation of **CBZ**·**SAC**·MeOH, and we conducted an extensive screen for SpeedMixing cocrystallization of **CBZ** and **SAC** with either anhydrous MeOH, or specific MeOH:H<sub>2</sub>O mixtures as the liquid additive, at a range of  $\eta$ -values. The screen (Table I, also SI) also showed that the presence of water can be used to drive the selective SpeedMixing synthesis of either Form I or Form II **CBZ**·**SAC** polymorphs within 3 minutes. Specifically, MeOH with a low water content led to reproducible appearance of Form I, while increased water amounts produced the metastable Form II. Finally, high water contents produced the hydrate **CBZ**·2H<sub>2</sub>O. In all cases, SpeedMixing for 5 minutes or longer led only to Form I (Figure 3).

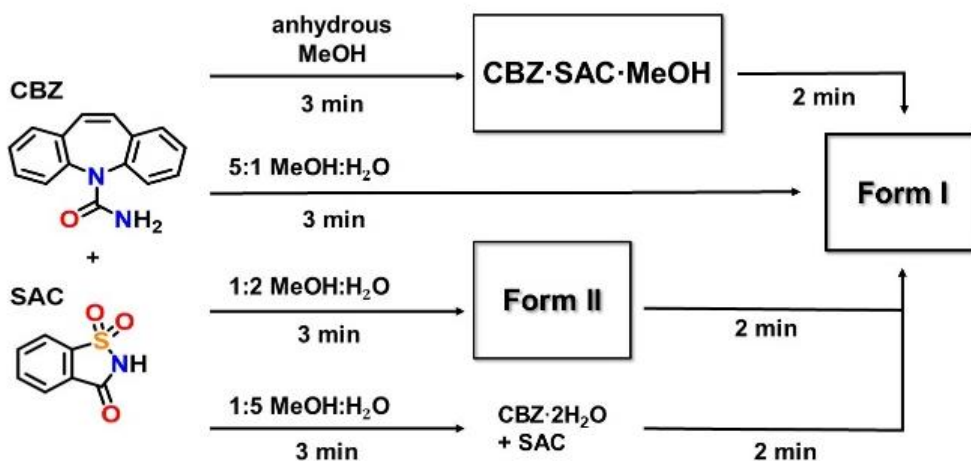


**Figure 3.** Schematic overview of transformations of **CBZ** and **SAC** by liquid-assisted SpeedMixing in the presence of MeOH or MeOH:H<sub>2</sub>O mixtures, producing **CBZ**·**SAC** Forms I or II, **CBZ**·**SAC**·MeOH, or **CBZ**·2H<sub>2</sub>O.

Next, we explored the applicability of SpeedMixing to selectively synthesize cocrystals composed of identical components, but in different stoichiometric ratios (stoichiometric variations, stoichiomorphs).<sup>23</sup> As a model we selected the well-known system of **NIC** and suberic acid (**SUB**).<sup>24</sup> The two components are known to form cocrystals of compositions **NIC**·**SUB** and **2NIC**·**SUB** (CSD NUKZAV01, NUKZES01, respectively). Varying the time and  $\eta$ -value revealed that each cocrystal can be accessed selectively and in complete conversion by SpeedMixing in the presence of MeOH ( $\eta = 1.54 \mu\text{L}/\text{mg}$ ) of the components in appropriate stoichiometric ratio within 45 minutes, *i.e.* through six consecutive cycles of SpeedMixing (Figure 4). The cocrystals readily formed even at much shorter SpeedMixing times, *e. g.* 1 minute, but at incomplete conversion.

Shorter SpeedMixing was also found to generate mixtures of **NIC·SUB** and **2NIC·SUB**, regardless of the initial reaction mixture composition. This observation distinguishes SpeedMixing from ball milling, where **NIC·SUB** appears as an intermediate in the formation of **2NIC·SUB**, while milling synthesis of **NIC·SUB** proceeds without an intermediate.<sup>25</sup> This suggests that cocrystallisation occurs via a deliquescence mechanism similar to that in accelerated ageing,<sup>26</sup> where different stoichiomorphs can be initially seen, but eventually all interchange into the one whose composition reflects that of the starting reaction mixture.

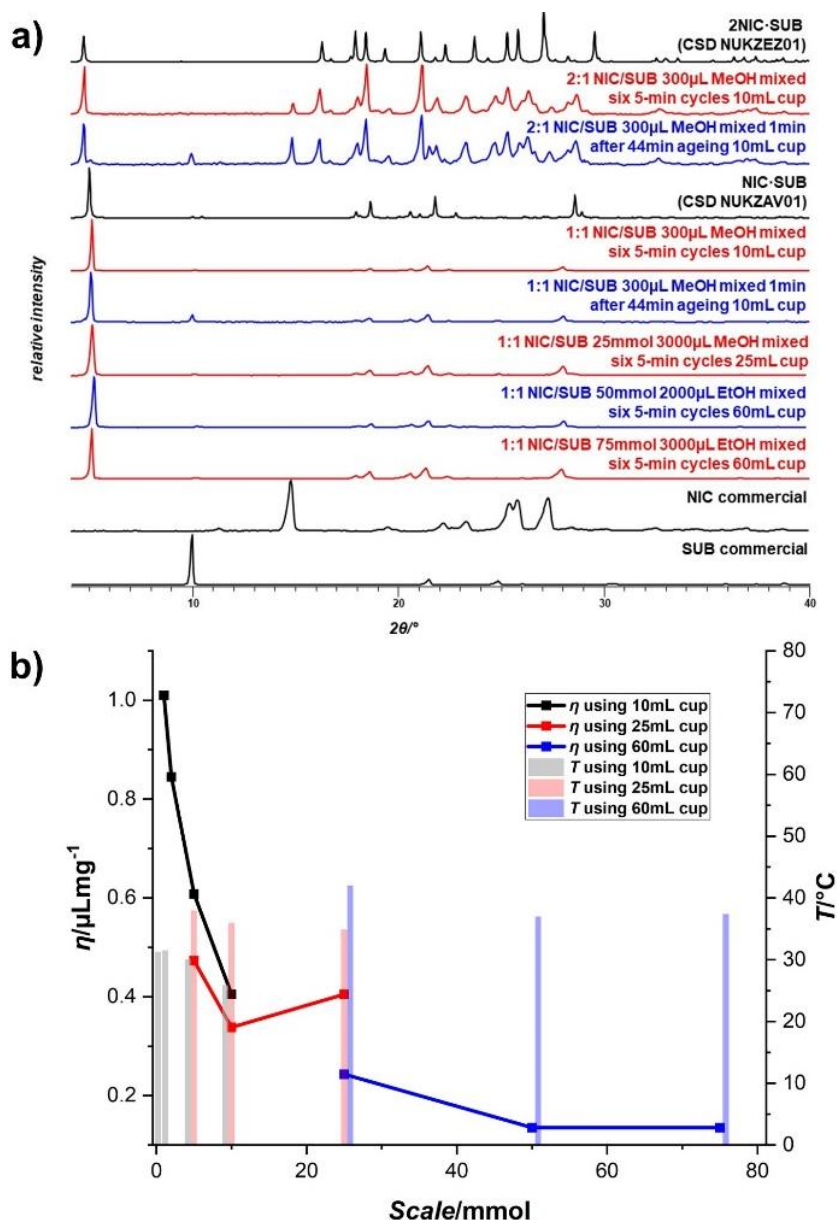


**Figure 4.** (a) Selected PXRD patterns illustrating the selective synthesis and scaling-up of stoichiometric variations of the **NIC·SUB** cocrystal (top-to-bottom): simulated for **2NIC·SUB** (CSD NUKZEZ01); a 2:1 stoichiometric mixture of **NIC** and **SUB** (1 mmol scale) after SpeedMixing for six 5-min cycles; a 2:1 stoichiometric mixture of **NIC** and **SUB** (1 mmol scale) after SpeedMixing for 1 min and static ageing for 44 min; simulated for **NIC·SUB** (CSD NUKZAV01); a 1:1 stoichiometric mixture of **NIC** and **SUB** (1 mmol scale) after SpeedMixing for six 5-min cycles, 1:1 stoichiometric mixture of **NIC** and **SUB** (1 mmol scale) after SpeedMixing for 1 min and ageing for 44 min; a 1:1 stoichiometric mixture of **NIC** and **SUB** (25 mmol scale) after SpeedMixing for six 5-min cycles in a 25 mL cup; a

1:1 stoichiometric mixture of **NIC** and **SUB** (50 mmol scale) after SpeedMixing for six 5-min cycles in a 60 mL cup; a 1:1 stoichiometric mixture of **NIC** and **SUB** (75 mmol scale) after SpeedMixing for six 5-min cycles in a 60 mL cup. (b) Comparison of  $\eta$ -values (lines) and final temperature (vertical bars) for experiments leading to full conversion into **NIC·SUB** at different scales, using MeOH (10 mL, 25 mL cup) or EtOH (60 mL cup) as the liquid additive.

Finally, we addressed the possibility of scaling-up SpeedMixing cocrystallization with **NIC·SUB** as a model. Systematic variation of mixing cup sizes and  $\eta$ -values enabled a ca. 70-fold scaling-up of synthesis, from 300 mg to 22 g, using a 60 mL cup in a procedure consisting of six periods of SpeedMixing. The systematic exploration of reaction conditions also revealed that the  $\eta$ -value required for complete conversion into **NIC·SUB**, based on PXRD analysis, decreases with an increase in reaction scale. Consequently, cocrystal formation by liquid-assisted SpeedMixing appears to become increasingly efficient at larger scales, and required less liquid additive. The increase in efficiency could also be related to a mild increase in the reaction mixture temperature at larger scales: measuring the temperature of the mixing cup immediately after SpeedMixing using an infrared thermometer<sup>27</sup> revealed temperatures around 28-30 °C for reactions in a 10 mL cup, and 37-42 °C when using a 60 mL cup (Figure 4b). This exploration also reveals that increasing the amount of material to occupy more than ca. one-third of the SpeedMixing cup leads to poorer reactivity and loss of homogeneity. This problem was overcome either by increasing the  $\eta$ -value (Figure 4b) or by using a larger cup. The latter approach, however, led to more significant evaporation of the liquid additive which was countered by replacing MeOH with EtOH.

## Conclusions

We have demonstrated the use of the dual asymmetric centrifugal mixing (SpeedMixing), initially developed for blending of viscous and soft materials, as a route to conduct rapid, controllable synthesis, and even discovery, of solid API forms. SpeedMixing cocrystallisation operates without bulk solvents, using conditions typically found in liquid-assisted mechanochemistry, but without grinding or milling media. Compared to other emergent solvent-free, media-free approaches for synthesis and discovery of solid API forms, *e.g.* accelerated aging, acoustic mixing or vapor-assisted tumbling, SpeedMixing is rapid, enables small-scale experiments within 3-5 minutes, and syntheses at tens of grams scale within 45 minutes. We show that SpeedMixing also permits the selective synthesis of stoichiomorphs, polymorphs, and also solvates of APIs or API cocrystals. In that context, the discovery of the first solvate of the archetypal pharmaceutical cocrystal **CBZ·SAC**, and the ability to selectively obtain polymorphic **CBZ·SAC** Forms I and II, highlight SpeedMixing as a rapid, simple and 'soft' route for the synthesis and discovery of new pharmaceutical forms, even in previously already well-explored cocrystal systems.

## Acknowledgements

We thank Mr D. Liu and Ms K. Sears at the Facility for Electron Microscopy Research of McGill University for help in microscope operation and data collection. Dr R. S. Stein is acknowledged for providing NMR data.

## References

1) a) D. Hasa, W. Jones, *Adv. Drug. Deliv. Rev.* **2017**, *117*, 147-161; b) V. Declerck, P. Nun, J. Martinez, F. Lamaty *Angew. Chem. Int. Ed.* **2009**, *48*, 9318-9321; c) C. Bolm, J. G. Hernández

*Angew. Chem. Int. Ed.* **2019**, *58*, 3285-3299; d) D. Tan, L. Loots, T. Friščić, *Chem. Commun.* **2016**, *52*, 7760-7781; e) D. Braga, L. Maini, F. Grepioni, *Chem. Soc. Rev.* **2013**, *42*, 7638–7648.

2) a) Q. Cao, J. L. Howard, D. E. Crawford, S. L. James, D. L. Browne *Green Chem.* **2018**, *20*, 4443-4447; b) J. Andersen, J. Mack. *Chem. Sci.* **2018**, *20*, 1435-1443; c) J. G. Hernández, C. Bolm *J. Org. Chem.* **2017**, *82*, 4007-4019.

3) a) J. L. Howard, Q. Cao, D. L. Browne *Chem. Sci.* **2018**, *9*, 3080-3094; b) D. R. Weyna, T. Shattock, P. Vishweshwar, M. J. Zaworotko, *Cryst. Growth Des.* **2009**, *9*, 1106-1123; c) O. Galant, G. Cerfeda, A. S. McCalmont, S. L. James, A. Porcheddu, F. Delogu, D. E. Crawford, E. Colacino, S. Spataro *ACS Sustainable Chem. Eng.* **2022**, *10*, 1430-1439; d) F. Puccetti, S. Lukin, K. Užarević, E. Colacino, I. Halasz, C. Bolm, J. G. Hernández *Chem. Eur. J.* **2022**, *28*, e202104409; e) S. K. Rai, A. Gunnam, M. K. C. Mannava, A. K. Nangia *Cryst. Growth Des.* **2020**, *20*, 1035-1046.

4) T. Friščić, S. L. Childs, S. A. A. Rizvi, W. Jones *CrystEngComm* **2009**, *11*, 418-426; b) P. Ying, J. Yu, W. Su, *Adv. Synth. Catal.* **2021**, *363*, 1246-1271; d) G. A. Bowmaker, *Chem. Commun.* **2013**, *49*, 334-348; c) D. Hasa, G. S. Rauber, D. Voinovich, W. Jones, *Angew. Chem.* **2015**, *54*, 7371-7375.

5) a) E. Boldyreva, *Chem. Soc. Rev.* **2013**, *42*, 7719–7738; b) D. Tan, F. García, *Chem. Soc. Rev.* **2019**, *48*, 2274–2292; c) G.-W. Wang, *Chem. Soc. Rev.* **2013**, *42*, 7668–7700; d) R. T. O’Neill, R. Boulatov, *Nat. Chem. Rev.* **2021**, *5*, 148–167; e) N. R. Rightmire, T. P. Hanusa, *Dalton Trans.* **2016**, *45*, 2352–2362; f) A. A. L. Michalchuk, F. Emmerling *Angew. Chem. Int. Ed.* **2022**, e202117270.

6) a) A. Sato, J. Kano, F. Saito, *Adv. Powder Technol.* **2010**, *21*, 212-216; b) D. Steiner, J. H. Finke, S. Breitung-Faes, A. Kwade, *Adv. Powder Technol.* **2016**, *27*, 1700-1709; c) M. F. Franco, R. Gadioli, M. A. D. Paoli, *Polímeros* **2019**, *29*.

7) a) D. Braga, S. L. Giaffreda, F. Grepioni, M. R. Chierotti, R. Gobetto, G. Palladino, M. Polito, *CrystEngComm* **2007**, *9*, 879-881; b) I. Huskić, C. B. Lennox, T. Friščić, *Green. Chem.* **2020**, *22*, 5881-5901; c) C. A. O’Keefe, C. Mottillo, J. Vainauskas, L. Fábíán, T. Friščić, R. W. Schurko, *Chem. Mater.* **2020**, *32*, 4273-4281; d) X. Feng, C. Jia, J. Wang, X. Cao, P. Tang, W. Yuan, *Green. Chem.* **2015**, *17*, 3740-3745; e) A. J. Stirk, F. E. S. Souza, J. Gerster, F. M. Mir, A. Karadeolian, A. W. Rey, *Green. Chem.* **2022**, *24*, 1505-1514.

8) a) G. Beniah, B. E. Uno, T. Lan, J. Jeon, W. H. Heath, K. A. Scheidt, J. M. Torkelson, *Polymer* **2017**, *110*, 218-227; b) Y. Wang, J. Yu, W. Dai, Y. Song, D. Wang, L. Zeng, N. Jiang, *Polym. Compos.* **2015**, *36*, 556-565; c) S. Agate, P. Tyagi, V. Naithani, L. Lucia, L. Pal, *ACS Sustain. Chem. Eng.* **2020**, *8*, 1850-1858; d) D. P. Vanderbilt, B. Adams, K. L. Walker, H. Huang, D. V. Ruscio (Bausch & Lomb Inc.), US0002681, **2007**; e) N. Chergui, M. Lateb, É. Lacroix, L. Dufresne *Chem. Eng. Res. Des.* **2015**, *102*, 100–115.

9) M. B. Hickey, M. L. Peterson, L. A. Scoppettuolo, S. L. Morrisette, A. Vetter, H. Guzmán, J. F. Remenar, Z. Zhang, M. D. Tawa, S. Haley, M. J. Zaworotko, Ö. Almarsson *Eur. J. Pharm. Biopharm.* **2007**, *67*, 112-119.

10) For examples of diverse studies that relied on **CBZ·SAC** system as a model, see: a) J. J. Du, S. A. Stanton, S. Fasih, B. A. Hawkins, P. A. Williams, P. W. Groundwater, J. Overgaard, J. A. Platts, D. E. Hibbs *Cryst. Growth Des.* **2021**, *21*, 4259-4275; b) M. Omori, K. Sugano *Cryst. Growth Des.* **2021**, *21*, 6237-6244; c) L. M. Padrela, B. Castro-Dominguez, A. Ziaee, B. Long, K. M. Ryan, G. Walker, E. J. O’Reilly *CrystEngComm* **2019**, *21*, 2845-2848; d) S. K. Pagire, N. Jadav, V. R. Vangala, B. Whiteside, A. Paradkar *J. Pharm. Sci.* **2017**, *106*, 2009-2014; e) M. K. Corpinot, R. Guo, D. A. Tocher, A. B. M. Buanz, S. Gaisford, S. L. Price, D.-K. Bučar *Cryst. Growth Des.* **2017**, *17*, 827-833.

- 11) a) D. Prat, A. Wells, J. Hayler, H. Sneddon, C. R. McElroy, S. Abou-Shehada, P. J. Dunn, *Green. Chem.* **2016**, *18*, 288-296; b) P. J. Dunn, *Chem. Soc. Rev.* **2012**, *41*, 1452-1461; c) C. Jimenez-Gonzalez, D. J. Constable, C. S. Ponder, *Chem. Soc. Rev.* **2012**, *41*, 1485-1498; d) K. Grodowska, A. Parczewski, *Acta Pol. Pharm.* **2010**, *67*, 3.
- 12) S. G. Fleischman, S. S. Kuduva, J. A. McMahon, B. Moulton, R. D. Bailey Walsh, N. Rodríguez-Hornedo, M. J. Zaworotko, *Cryst. Growth Des.* **2003**, *3*, 909-919.
- 13) W. W. Porter III, S. C. Elie, A. J. Matzger, *Cryst. Growth Des.* **2008**, *8*, 14-16.
- 14) Conquest Version 2022.1.0, CSD Version 5.43 (November 2021).
- 15) G. R. Fulmer, A. J. M. Miller, N. H. Sherden, H. E. Gottlieb, A. Nudelman, B. M. Stoltz, J. E. Bercaw, K. I. Goldberg, *Organometallics* **2010**, *29*, 2176-2179.
- 16) a) M. C. Etter, J. C. MacDonald, J. Bernstein, *Acta Crystallogr. B* **1990**, *46*, 256-262; b) G. R. Desiraju *Angew. Chem. Int. Ed.* **1995**, *34*, 2311-2327.
- 17) S. Lohani, Y. Zhang, L. J. Chyall, P. Mougín-Andrés, F. X. Müller, D. J. W. Grant *Acta Cryst.* **2005**, *E61*, o1310-1312.
- 18) A. J. Cruz-Cabeza, G. M. Day, W. D. S. Motherwell, W. Jones *J. Am. Chem. Soc.* **2006**, *128*, 14466-14467.
- 19) For the phase diagram for the system of **CBZ**, **SAC** and MeOH, see: a) M. A. Oliveira, M. L. Peterson, R. J. Davey, *Cryst. Growth Des.* **2011**, *11*, 449-457; b) S. Kudo, H. Takiyama *J. Cryst. Growth* **2014**, *392*, 87-91; c) S. Kudo, H. Takiyama *J. Chem. Eng. Data* **2018**, *63*, 451-458.
- 20) a) M. M. Haskins, M. J. Zaworotko, *Cryst. Growth Des.* **2021**, *21*, 4141-4150; b) G. Di Profio, V. Grosso, A. Caridi, R. Caliandro, A. Guagliardi, G. Chita, E. Curcio, E. Drioli, *CrystEngComm* **2011**, *13*, 5670-5673; c) M.-J. Lee, I.-C. Wang, M.-J. Kim, P. Kim, K.-H. Song, N.-H. Chun, H.-G. Park, G. J. Choi, *Korean J. Chem. Eng.* **2015**, *32*, 1910-1917; d) I.-C. Wang, M.-J. Lee, S.-J. Sim, W.-S. Kim, N.-H. Chun, G. J. Choi *Int. J. Pharm.* **2013**, *450*, 311-322.
- 21) N. Schultheiss, A. Newman, *Cryst. Growth Des.* **2009**, *9*, 2950-2967.
- 22) The unexpected nature of **CBZ·SAC·MeOH** discovery is illustrated by a report of a previous high-throughput screen which also included MeOH:<sup>21</sup> "...in the case of the 1:1 cocrystal of carbamazepine and saccharin (Form I), an extensive polymorphic screen was conducted on one form. By means of high-throughput crystallization, 480 experiments including saccharin and carbamazepine in various solvents and solvent mixtures were performed, yielding 156 solid materials which were characterized by XRPD or Raman spectroscopy. No polymorphic forms of the cocrystal were observed. Additionally, solvent-assisted mechanical grinding experiments were tried, using 24 different solvents. The remaining solids were characterized by XRPD, resulting, once again, in only the original cocrystal form."
- 23) a) M. Arhangel'skis, F. Topić, P. Hindle, R. Tran, A. J. Morris, D. Cinčić, T. Friščić, *Chem. Commun.* **2020**, *56*, 8293-8296; b) T. Carstens, D. A. Haynes, V. J. Smith, *Cryst. Growth Des.* **2020**, *20*, 1139-1149.
- 24) S. Karki, T. Friščić, W. Jones, *CrystEngComm* **2009**, *11*, 470-481.
- 25) I. Halasz, A. Puškarić, S. A. J. Kimber, P. J. Beldon, A. M. Belenguer, F. Adams, V. Honkimäki, R. E. Dinnebier, B. Patel, W. Jones, V. Štrukil, T. Friščić, *Angew. Chem. Int. Ed.* **2013**, *52*, 11538-11541.
- 26) a) I. Huskić, J. C. Christopherson, K. Užarević, T. Friščić, *Chem. Commun.* **2016**, *52*, 5120-5123; b) C. Maheshwari, A. Jayasankar, N. A. Khan, G. E. Amidon, N. Rodríguez-Hornedo *CrystEngComm* **2009**, *11*, 493-500; c) H. Veith, C. Luebbert, N. Rodríguez-Hornedo, G. Sadowski *Cryst. Growth Des.* **2021**, *21*, 4445-4455.

27) a) H. Kulla, M. Wilke, F. Fischer, M. Röllig, C. Maierhofer, F. Emmerling, *Chem. Commun.* **2017**, *53*, 1664-1667; b) K. Kubota, Y. Pang, A. Miura, H. Ito, *Science* **2019**, *366*, 1500-1504.